A scotophobic response characterised by body contraction and ciliary arrest in *Acropora* coral larvae

Emelie A. Brodrick[1,2,3*], Kei Jokura[1,2,4,5], Jamie Craggs[6], Rebecca Poon[1,7], Hannah Laeverenz-Schlogelhofer[1,7], Kirsty Y. Wan[1,7], Gáspár Jékely[1,2,8,*]

[1]Living Systems Institute, University of Exeter, Exeter EX4 4QD, UK
[2]Biosciences, Faculty of Health and Life Sciences, University of Exeter, Exeter EX4 4QD, UK
[3]Sussex Neuroscience, School of Life Sciences, University of Sussex, Brighton, UK
[4]National Institute for Basic Biology (NIBB), Okazaki, 444-8585, Japan
[5]Exploratory Research Center on Life and Living Systems (ExCELLS), Okazaki, 444-8787, Japan
[6]Horniman Museum & Gardens, London SE23 3PQ
[7]Department of Mathematics and Statistics, University of Exeter, Exeter EX4 4QD, UK
[8]Heidelberg University, Centre for Organismal Studies (COS), 69120 Heidelberg, Germany
[*]**Correspondence: e.a.brodrick@sussex.ac.uk, gaspar.jekely@cos.uni-heidelberg.de**

Abstract

The motile planula larva of the reef-building coral *Acropora millepora* exhibits a distinct scotophobic response characterized by full-body contraction and ciliary arrest when exposed to abrupt light dimming. Through behavioural assays, we confirmed reductions in larval swimming speed and alterations in vertical and horizontal movement patterns under alternating light and dark conditions. High-speed microscopic imaging revealed that ciliary activity ceases upon light dimming, while the body contracts into a rounded shape, influencing swimming behaviour. These responses suggest an adaptive mechanism for maintaining optimal positioning within the highly structured and complex light environment of reef habitats, critical for coral recruitment and survival.

Introduction

The planula larva plays a critical role in the life cycle of a reef-building coral by dispersing from the parent colony. Within days of fertilisation and embryonic development, the larva must locate a suitable habitat to attach to, where it will settle and metamorphose into the primary polyp of a new coral colony. The animal will spend the rest of its life in that location, filter-feeding with tentacles (mostly at night), and using organic products of algal endosymbiont photosynthesis that are accrued during daytime [1]. Coral colonies can grow larger by producing clonal polyps via asexual budding.

Corals (Anthozoa, Hexacorallia, Scleractinia) are cnidarians, the sister group to all bilaterians [2,3]. The nerve net systems of both larvae and adults are not centralised into a brain-like structure, rather their nervous systems resemble nets or rings (particularly in medusoid forms), across their rotationally-symmetric bodies [4]. Members of this deep-branching animal phylum have nervous systems with specialised sensory neurons and interneurons. Planula larvae have a nerve plexus at the anterior aboral pole, which usually underlies an apical organ of sensory cells. Despite the relative simplicity or seeming

disorganization in the nervous system, coral larvae can make decisions and are known to actively explore the substrate, choosy in where they settle [5–7]. They have been shown to use a multitude of sensory cues to inform their decision for successful settlement (reviewed in [8]).

Abundance of light in clear and relatively shallow water is an essential requirement for successful recruitment for corals with photosynthetic endosymbionts. The distribution of tropical coral-reef species often shows distinct zonation with depth [9,10]. The staghorn coral *Acropora millepora* has relatively large (500-900 μm long) lipid-filled larvae, which swim slowly and do not acquire endosymbionts until after metamorphosis into a polyp [11]. Anthozoan cnidarians lack visual eyes or any recognizable ocular structures in any stage of their life cycle. However, light intensity and its spectral properties are known to be important cues for larval settlement [9,12–16]. So, larval light-sensing is crucial to survival and ecological success of many reef-building coral species.

Adult *A. millepora* corals sense light using non-visual cryptochromes [17,18] and opsins [19,20] to monitor solar and lunar cycles. This information is used to time behaviours associated with nocturnal tentacle feeding and to synchronise annual spawning events [21]. The motile planula larvae of many scleractinian corals are also responsive to light. At least six light-sensitive opsin (Acropsin) genes have been identified so far from the larva of *A. millepora* [22,23]. However, the corals do not have specialised cells with distinctive morphology typical of ocellar photoreceptor cells, e.g. extensive microvillar or ciliary membrane elaborations and association with shading pigment. Rather, the opsin-expressing photoreceptor cells are scattered inconspicuously along the larval ectoderm and present similar shape and structure to neighbouring epithelial cells, making them difficult to identify using morphological analysis via electron microscopy.

In accordance with the expression of several opsins [23], coral larvae can show light-regulated behavioural responses including photomovement [24] or alleged phototaxis [25,26] in some species, and spectral preferences for settlement sites [9,13,15]. Notably, Sakai and colleagues [27] demonstrated reductions in average swimming speed within batches of *A. tenuis* larvae that were roughly proportional to the white light intensity-decrease that they were exposed to. They further tested the response with different wavelengths of light, showing that swimming speed is most affected by changes in blue light intensity, while not responsive to changes in red light. Here, we examine responses of *A. millepora* larvae to light dimming in further detail. We confirmed the presence of this light-off or scotophobic ("fear" of darkness) response in this species and also found that the coral larvae undergo whole-body muscular contraction in addition to ciliary arrest after a sudden dimming in light intensity. We propose a simple model for position maintenance in the water column and on the reef, in the absence of spatial vision.

Materials and Methods

Colonies of *ex situ A. millepora* synchronously spawned (1 Dec 2021 & 14 Nov 2022) at the Horniman Museum and Gardens Aquarium facility, London, UK. The gametes from different colonies were cross-fertilised to produce embryos, which were transported to University of Exeter, UK when they were 3 days post fertilisation (dpf) and our experiments were carried out between 5 and 7 dpf. Larvae were stored in 500 ml covered glass containers in seawater at 27 °C inside an incubator, with aquarium lighting (Marine 3.0 Nano, Fluval, Quebec, Canada) providing a 12/12 hr light/dark cycle.

Unless specified, all experiments were carried out in a 27 °C temperature-controlled room to prevent temperature fluctuations and all experiments were conducted in a dark room with no external sources of visible light.

Light spectra were measured from each experimental apparatus (Fig. S1 A-D) from the position that larvae were held, in absolute irradiance using a calibrated spectrophotometer (QE65000, Ocean Optics, Orlando, USA) coupled to an optical fibre and cosine corrector. The total absolute irradiance from a light source was then attained by calculating the area under the spectrum curve.

Free-swimming horizontal assays

Larvae (*n*=10-15) were placed in a 5 mm shallow glass cuvette (20 x 9 mm) containing 900 µl seawater and allowed to swim freely (apparatus depicted in Fig. 1A). They were recorded using an infrared-sensitive USB camera (iDS UI-3360CP-M-GL Rev.2, Imaging Development Systems, Obersulm, Germany) mounted on a stereomicroscope (Leica M205, Wetzlar, Germany). An infrared ring light (LED-HP6095-3, LeeTun Optical Tools, China) with peak emission at 850 nm wavelength was positioned below to create dark-field illumination, with absolute irradiance of 2543.7 µW/cm^2/nm. A 780 nm long-pass colour filter (FGL780S, Thorlabs, Newton, NJ, USA) was placed in front of the camera to stabilize the image during light stimulus changes.

Light stimulation was provided from one side (which alternated) during the first 90 s using a white LED (MCWHL7, Thorlabs, Newton, NJ, USA) controlled with an LED driver (LEDD1B, Thorlabs, Newton, NJ, USA). The beam was passed through a collimating lens (LAG-65.0–53.0 C with MgF2 Coating, CVI Melles Griot) to produce a bright (5 cm diameter) spot of light with uniform intensity to fill the whole area of the cuvette. Larvae were first acclimatized to the bright light for 5 minutes, with total absolute irradiance of 1421.6 µW/cm^2/nm. Starting with the stimulation light on, 90-second alternating photoperiods (light on/off) were shown twice, making a total experiment time of 6 minutes. Experiments were carried out in an otherwise dark room so that there was no visible light available to the larvae during the light-off periods, resulting in measured absolute irradiance 0.0 µW/cm^2/nm (spectral data in Supplementary Fig. S1A).

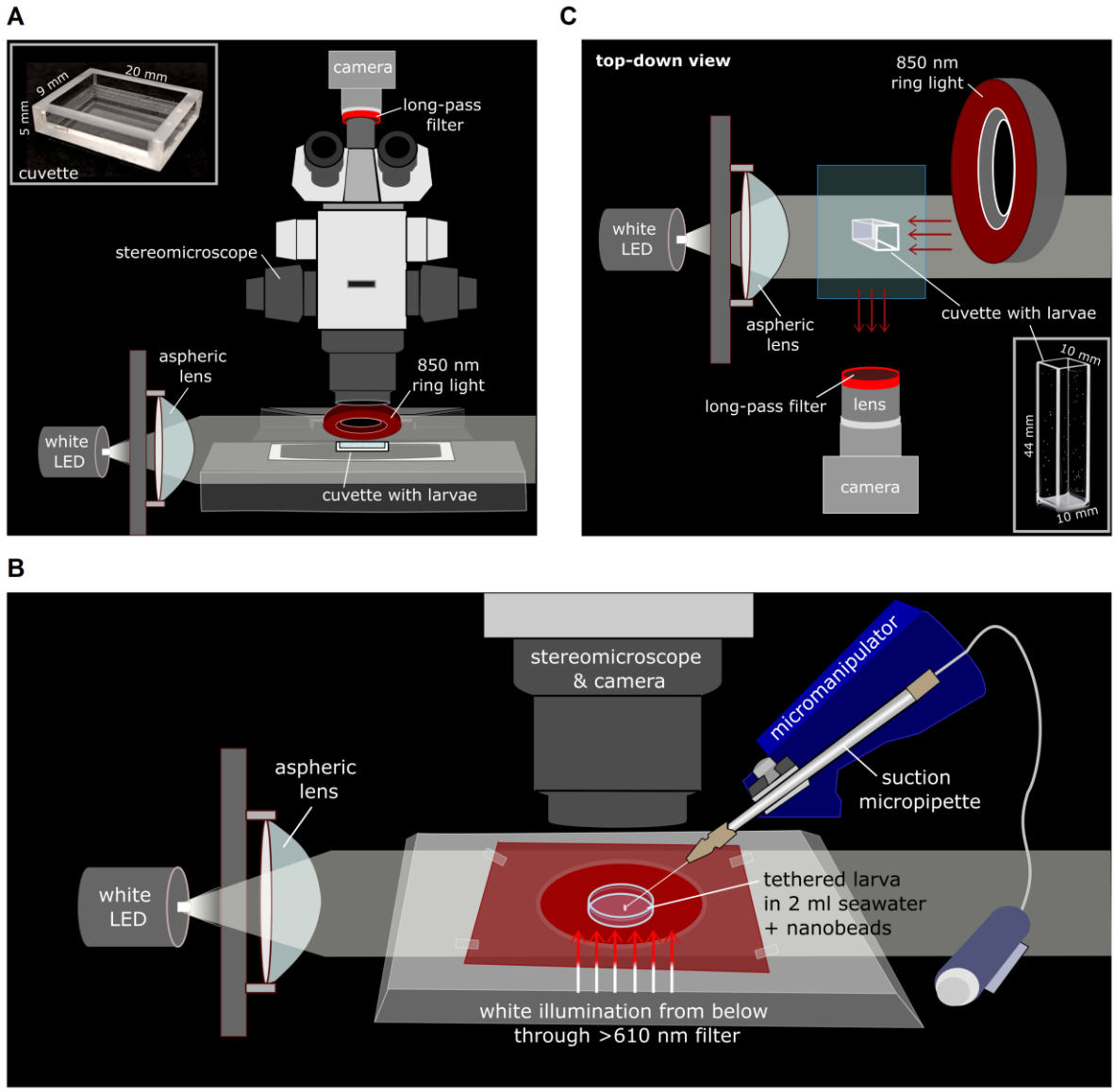

Fig. 1. Schematics of the apparatus used to assess photobehaviour. A) *Free-swimming larvae held in a shallow cuvette to assess horizontal movement in response to white light on/off stimulation.* ***B)*** *Top-down view of apparatus used to assess vertical movements of free-swimming larvae inside a 44 mm high cuvette.* ***C)*** *A single larva is tethered on a suction micropipette and held in a dish of seawater containing nano-particle beads that allow visualization of flow fields and measurement of bodily shape changes.*

Video data from six repeats of the experiment were run and were analysed with a custom Fiji macro , which used the Mtrack2 plugin (Stuurman, 2003, https://valelab4.ucsf.edu/~nstuurman/IJplugins/MTrack2.html). The video was sampled into 5 sec (100 frame) clips and from each clip, xy coordinates of thresholded larval profiles were extracted between video frames. Custom scripts in R (version 4.1.3 [28]) were used to analyse the data, then calculate and plot swimming speed, in addition to swimming

trajectories with respect to the direction of the light source. To allow for adjustments in behaviour to ensue, speed and horizontal displacement data from the second 45 s half of each time period were compared statistically with Mann-Whitney Wilcoxon rank sum tests, due to non-normality within the datasets (Shapiro-Wilk tests, $p<0.05$). All analysis code, source data and video for this manuscript is available at: 10.5281/zenodo.14810574

Body shape changes

Data were collected over two years, a Year 1 cohort (2021, n=6) and a Year 2 cohort (2022, n=7). One at a time, larvae were held in a 30 mm diameter petri dish of filtered seawater under a Leica M205 stereomicroscope. A custom-pulled suction micropipette (TW-1200 borosilicate glass) attached to a micromanipulator was used to tether the larvae from the side or near the oral pole. White light from below the dish was passed through a film of red long-pass filter (>610 nm), providing constant illumination for the field of view. Red light was used rather than near-infrared in this instance so that nanobeads could be visualized effectively to assess ciliary flowfields (details in next section). Video data were collected through a 620 nm long-pass colour filter by a USB camera (iDS UI-3360CP-M-GL Rev.2) with near-infrared sensitivity (apparatus depicted in Fig. 1C).

A cool-white mounted LED provided light stimulation from one side. The beam was passed through a collimating lens (as above). After tethering, each larva had an acclimatization period of 5 minutes with the LED light stimulation on, which is how the experiment video began. In Year 1, larvae were exposed to three alternating light-on/ light-off cycles. These were 90 s long, except for the first light-on period for which, only 30 s was recorded. In Year 2, the larvae were shown just two on-off light cycles of 90 s each. Light intensity was kept the same between the two years (spectral data in Supplementary Fig. S1B).

Larval profiles were measured from thresholded images with standard built-in ImageJ functions and plugins. Planula length, width and body area were recorded from frames every 10 s in the videos. Body aspect-ratio was calculated by dividing body length by width and data from the second 45 s half of each time period were compared statistically with Mann-Whitney Wilcoxon rank sum tests, due to non-normality (Shapiro-Wilk tests, $p<0.05$). The same statistical tests were used to compare projected body area also.

Ciliary flowfields

The 6-minute videos from the 2022 dataset used to measure body shape changes were additionally analysed to assess flow fields created in the surrounding water by the larva's beating cilia (Fig. 1C). The seawater contained 1 µm Fluoresbrite® multifluorescent microspheres (volume fraction 10−5 v/v) to allow measurement of the flow fields and the video was captured at 90 fps. The videos were analysed with the PIVlab tooblox (v2.63) in MATLAB (2023b, MathWorks, Natick, MA, USA). After generating flow vectors, the mean velocity magnitude was measured from regions of fluid flanking the side of each larva between frames of the videos. The location of these areas were adjusted at times during the video to allow for larval shape changes and movement of the larva's position on the micropipette. The raw data were smoothed by averaging across each second (90 frames).

154 ## Ciliary beat frequency

155 Larvae were tethered with a custom-pulled TW-1200 borosilicate glass suction
156 micropipette (90/30 μm OD) attached to a micromanipulator and held in a dish of seawater
157 on a Leica DMi8 inverted microscope stage. Imaging was conducted at 22 °C room
158 temperature (because the microscope could not be moved to the 27 °C room). Video data
159 were collected from the microscope in Differential Interference Contrast (DIC) with 40x
160 objective (Leica HC PL FLUOTAR L 40x/0,60 CORR PH2) and a Phantom V1212 camera.
161 Regions of ectodermal locomotor cilia were recorded at 500 fps from previously light-
162 adapted larvae. The larvae were imaged under bright white light for about 30 s, then the
163 light was switched to dim red-filtered (>600 nm) light for the remainder of the recording
164 (spectral data in Supplementary Fig. S1C). The camera gain was increased by 4.5x to adjust
165 for the lowered light intensity.

166 The ciliary zone within each frame was located by thresholding the image to find the
167 boundary of the (opaque) larval body. The cilia project approximately 20 μm outwards
168 from the body surface. For each frame, multiple small boxes were drawn within the ciliary
169 band, parameterised by the arc length, *d.* The boxes extended 40 pixels (14.4 μm) in the
170 direction normal to the larval body surface, and 13 pixels (1.8 μm) in the *d* direction.
171 Within each box, the standard deviation of the image intensity was calculated for each
172 video frame, giving a time series at each location *d*. A wavelet transform was then
173 calculated from the time series at each value of *d* to give the time-resolved frequency
174 spectrum of the signal at that location. The magnitude of the wavelet transform was
175 averaged over the 6-12 Hz frequency band, since the periodic beating occurs at a frequency
176 of approximately 8-10 Hz. This value indicates how periodic the signal is as a function of
177 time, thus giving a high value when the cilia are beating, and a low one when they are
178 stationary. These averaged wavelet transforms of all of the locations are stacked to produce
179 kymographs.

180 ## Vertical positioning

181 Free-swimming larvae (4 dpf) were placed into a glass cuvette of seawater measuring 44
182 mm height (10 x 10 mm width and length) and illuminated from one side with the near-IR
183 ring light (apparatus depicted in Fig. 1B). The same infrared-sensitive camera with lens and
184 long-pass (780 nm) filter used in previous experiments captured video (20 fps) from
185 directly in front of the cuvette. On the opposite side of the IR ring light, a cool-white LED
186 passed through a collimating lens provided an even beam of light stimulation in 90-second
187 on/off photoperiods that repeated twice (6 minutes total). Light intensity values were kept
188 the same as in the horizontal swimming experiment (spectral data in Supplementary Fig.
189 S1D).

190 Video data were analysed to track the larvae's position using a similar method as described
191 for the first horizontal free-swimming larvae experiment (in shallow cuvette). Smaller time
192 intervals of 1 sec / 20 frames were used to track larvae to allow for the greater density of
193 animals and the higher frequency of track overlaps, preventing gross undersampling.

194 To assess the natural buoyancy of the larvae, the cilia were removed temporarily by
195 exposing larvae to hyperosmotic seawater (3% NaCl in seawater) for around 30 s until

swimming movements ceased. Larvae were washed in clean seawater immediately after. This deciliation method was reproduced from Takeda-Sakazume and colleagues [29]. The deciliated larvae were placed inside the vertical glass cuvette and recorded (with light stimulus on) on the camera (20 fps). The water was mixed by pipetting water up and down twice to redistribute the larvae in the water column. Then, trajectories of the larvae were recorded for 50 s as they moved inside the cuvette according to their buoyancy. The deciliated larvae were kept overnight to confirm that they were alive and healthy during the experiment. Observations the next morning confirmed not only survival, but that the larvae had regrown ectodermal cilia and were once more swimming as usual.

Statistical analyses were performed by comparing speed and vertical displacement data from the middle 30 s of each dark period with the middle 30 s of the second light period. Mann-Whitney Wilcoxon rank sum tests were performed due to non-normality of the data sets (Anderson-Darling tests, $p<0.05$).

Results

Larval swimming speed is reduced during dark periods

To assess whether *A. millepora* larvae display a similar light-off (scotophobic) swimming speed response to that of *A. tenuis,* (reported by [27]), free-swimming larvae (6 batches of 10-15 individuals, n=109) were tracked inside a shallow cuvette. Movement speed was assessed while the light stimulation conditions were alternated between 90 s white light (absolute irradiance 121.6 μW/cm²/nm) and 90 s darkness (0.0 μW/cm²/nm).

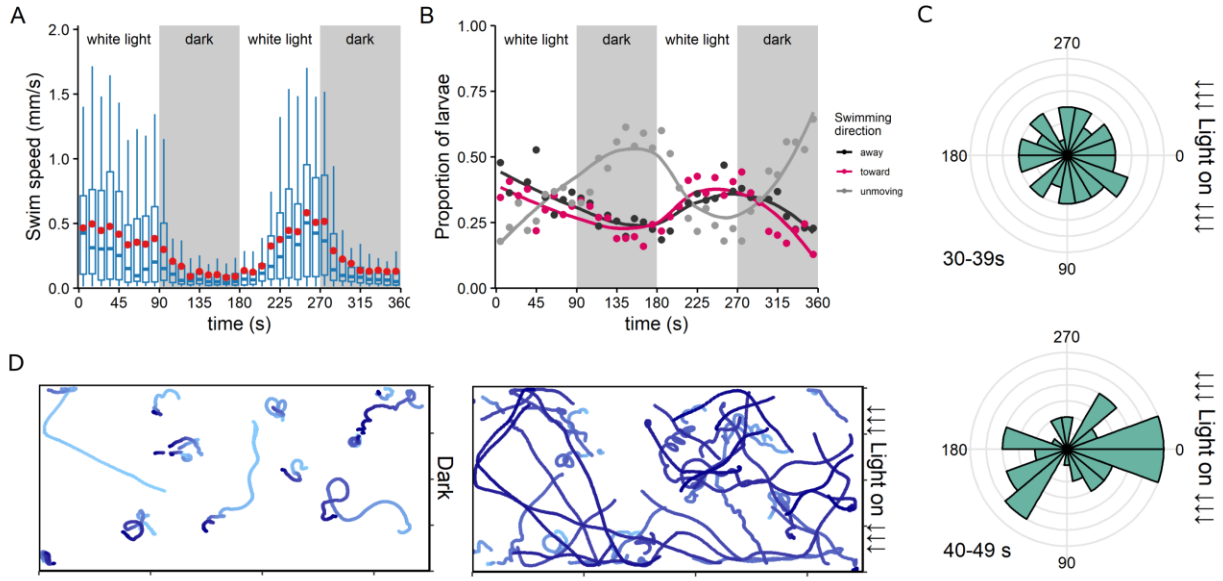

Figure 2. Free-swimming photobehaviour of A. millepora larvae in shallow cuvettes. *Light stimulation was provided in alternating 90 s intervals of collimated bright white light and darkness. Tracking of individual larval positions allowed measurement of* ***(A)*** *swimming speed represented as boxplots where horizontal bars show median values, while overlaid red points show mean.* ***(B)*** *Swimming direction as a proportion of the total number of larvae, with*

respect to position of the light source, averaged across six batches of 10-15 larvae. ***C****) The angle of larval trajectories over 10 s for all six batches are shown as circular histograms of 20-degree bin width. The data come from the second light-on period, 30-39 s and 40-49 s after the stimulus light came on. Those travelling at zero degrees (right) are moving directly towards the light source. Grey lines represent larval counts of 1.* ***D)*** *Example batch showing trajectories (x,y) of larvae over time in the first dark period (91-180 s) and following light-on period (181-270 s). Increasing time is represented by increasing darkness of the blue shade of the points. Dimensions of cuvette area are 20x9 mm.*

Under the initial phase of bright white light, the pre-light-adapted larvae swam at a mean speed ± its standard deviation of 0.41 ±0.43 mm/s, with maximum speed of 2.0 mm/s. Mean swimming speed was altered by the light changes (Fig. 2A, see Video S1 for example) and comparing the final 45 s (second half) of bright time periods with dark periods revealed a significant reduction in swimming speed in the dark (Wilcoxon rank sum test W=183558, $p<0.001$, Table S1 for full statistical test results and Fig. S2 for individual batch figures). Larval swimming speed reduced around 10 s after the onset of darkness, and during the final 60 s of the dark phase, it averaged 0.10 ±0.16 mm/s. In the following light phase, swimming recovered gradually until it reached a speed of 0.51 ±0.45 mm/s in the final 30 s of this light phase. Finally, larvae in the second dark phase showed a similar response to the first, with relatively rapid reduction of swimming speed (within 10-20 s), reaching a mean of 0.14 ±0.23 mm/s in the final 30 s.

Larvae showed no evidence of phototaxis

Swimming direction in a horizontal plane was not influenced by the position of the light source (Fig. 2B) and the proportion of larvae swimming towards or away from the light source remained equal to one another during the bright light periods. The proportion of larvae considered to be "unmoving" (travelling less than 0.1 mm/s in any direction) increased (to >0.5 of the total) during the second half of the dark periods. Comparing horizontal displacement in the second half (last 45 s) of each light condition, we found no difference between bright light and dark (Wilcoxon rank sum test W=338476, $p=0.273$, Table S2 for full statistical test results and Fig. S3 for individual batch figures).

Figure 2C shows the angles of larval trajectory over 10 s after the light stimulus came on the second time. We show here 30-39 s and 40-49 s after stimulus change because that is when most larvae began to actively swim and travel again in the cuvette after spinning on the spot during the dark phase. In both periods, larvae travelled in random directions with respect to the light source at 0°, especially between 30-39 s. It should be noted that due to the rectangular shape of the cuvette, it would be expected that there would be greater movement in the horizontal plane (0° and 180°), as is seen between 40-49 s. This shows that when light stimulation is presented after a dark period, larvae do not swim towards the light source. To visualise the difference in swimming behaviours, larval trajectories for one example batch (#2) are plotted for the entire first dark period and the following light period (Fig 2D). Supplemental Video S1 shows the movement trajectories for another batch (#3). The larvae tended to spin on their own axis in the dark, as shown by the small loops. In the following light-on phase, greater distances are covered in random directions.

Ciliary arrest and flowfields

Individual tethered larvae (*n*=6) were also examined more closely while ambient light conditions alternated between bright white light and dim red light. Using particle image velocimetry, we measured the flow of water movement from an area flanking the side of the larvae, created by the beating cilia of the larvae (Fig. 3, see video S2 for example of raw data). This allowed an indirect assessment of ciliary swimming activity.

Overall, fast active flow was recorded around larvae during light-on periods, then flow reduced or stopped completely during the dark phases (Fig. 3A & B, examples in Videos S2 & S3). There was a considerable range in adjacent water flow-speed between individuals under bright light conditions (0.5 - 1.0 mm/s) and flow speed fluctuated considerably over short timescale during light periods. One larva was not swimming actively during the first light phase, and two other larvae did not resume fast swimming in the second light-on phase. However, the flow reduction response to the decrease in white light intensity was consistent. The flow reduced to its minimum quickly, within 15 s after white light dimming (e.g. Fig. 3A) and in most cases sustained a very low speed until the following light phase. Similar to the trend in swimming speed, the recovery of fast slow in the second light phase was gradual compared to the light-off response (Fig. 3B).

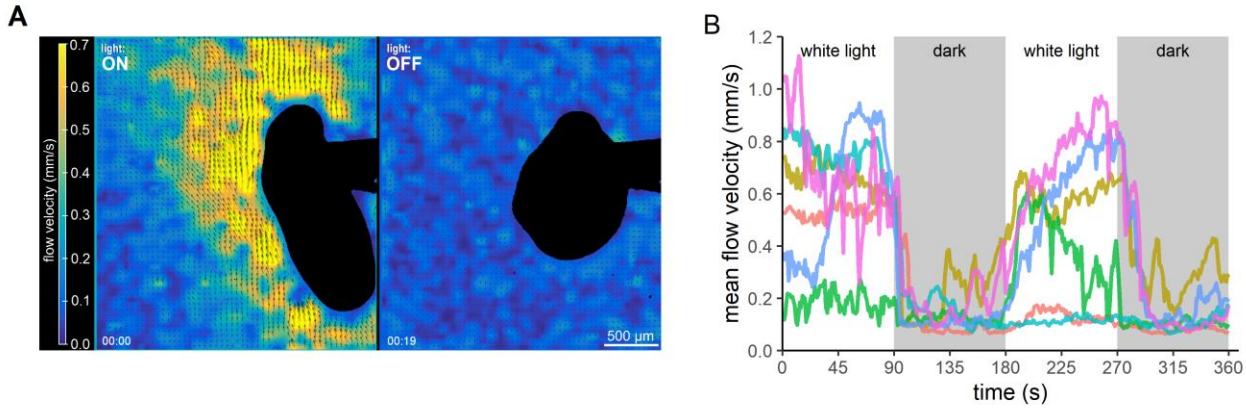

Figure 3. Flow velocity (mm/s) of water flanking tethered larvae. A) *Examples of PIV analysis showing active flow with white stimulus light on (left) and then 20 s later (right) when the stimulus light had been off for 15 s.* ***B)*** *Flow velocities for six individual larvae are represented in different colours over time as light intensity was alternated between bright white light and dim red light. The larvae create these flows with their swimming cilia and they are measured by particle image velocimetry using nanobeads in the water.*

To directly evidence ciliary arrest in response to change from bright white light to dim red light, we performed high-speed imaging at 500 fps of ectodermal swimming cilia from several larvae. Here, we illustrate two examples (Fig. 4), which show that although a ciliary arrest happens for both, the time between the change to dim red light and the stop in ciliary beating varies quite considerably, from around 4-43 s. Our first example (Larva #1), where an aboral pole region was imaged (Fig. 4Ai), the cilia show (slightly patchy) beating during the initial 30 s in bright light (Fig. 4Aii). Just 4 s after the switch to dim red light, all cilia stop their beating simultaneously, demonstrating a rapid scotophobic response (Fig.

296 4Ci, Video S4). After around 20 s of the red light condition, the cilia from *d*=200-370 μm
297 recovered and displayed intermittent beating, whilst the rest of the cilia remained
298 stationary for the rest of the imaging period (Fig. 4Aii).

299 Larva #2 was imaged nearer the oral pole (Fig. 4Bi) and the strength of the ciliary beat
300 frequency periodicity was weaker here (0.2, compared to 0.5 at the aboral region of larva
301 #1). The cilia here were slower to respond after the change to dim red light (Fig. 4Bii, Video
302 S5). The cilia at *d*=0 μm stopped beating first, 43 s after the stimulus light dimming. Then,
303 the arrest spread progressively across the ectoderm at a rate of 23.3 μm/s. It reached
304 *d*=166 μm around 7 s later, producing the sloped boundary seen in Fig. 4Cii. Soon after all
305 the cilia had stopped, those within the *d*=0-100 μm region recovered their beating, whereas
306 the other section of cilia (*d*=100-166 μm) remained motionless.

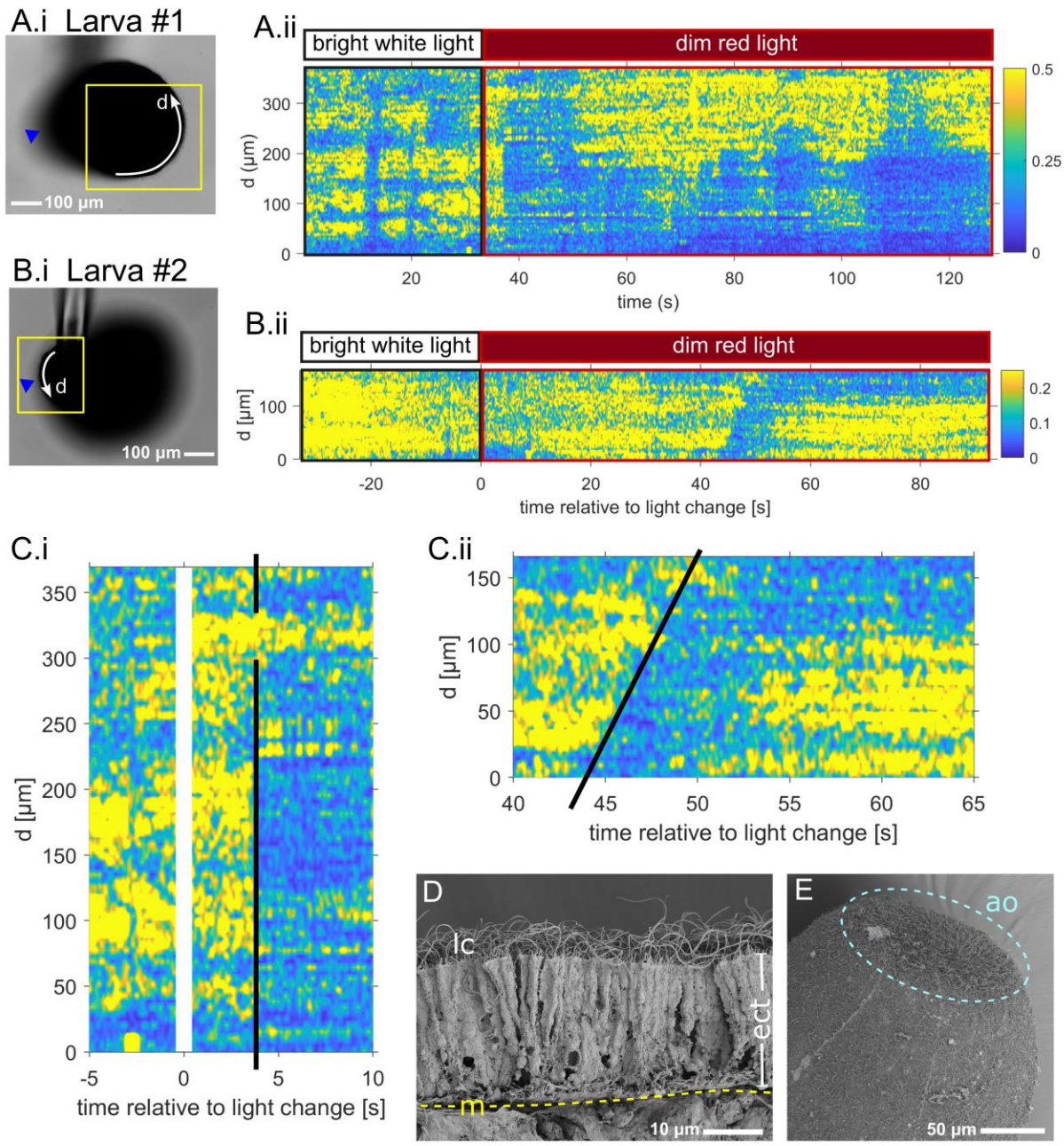

Figure 4. Ciliary beating responses of two individual larvae to light dimming revealed by high speed imaging. *Larva #1 (**Ai**) and Larva 2 (**Bi**) viewed with low magnification, tethered on the micropipette. Yellow boxes indicate the region of interest from which high-speed videos were recorded. Blue arrows show the location of the oral pores, so that Larva #1 shows data taken at the aboral/anterior end of the body, and Larva #2 at the oral/posterior end. The data are spatially resolved so within each video, different locations of the cilia around the larval body are parameterised by the arc length d, indicated by the white curved arrows. This region was limited to the section of the ciliary surface that was in focus.* ***Aii & Bii)*** *Kymographs showing the magnitude of the periodic signal from the ciliary surface of Larva #1 (Aii) and Larva #2 (Bii) during a light-off response experiment. The colour indicates*

strength of the periodic signal in the video as a function of arc length (d) along the edge of the larva and time (s) . A high value (yellow) means that the cilia are beating periodically, whilst a low value (blue) shows that the cilia are not beating. ***C)*** *The ciliary arrest response is shown in more detail, shortly (4 s) after the light dimming for larva #1 (i) and more than 40 s after the dimming for Larva #2 (ii). A black line indicates the pattern of arrest in space, d, along the edge of the larva.* ***D)*** *SEM image of the fractured ectoderm (ect) of a fixed A. millepora larva showing the dense locomotor cilia (lc) protruding from each long, narrow ectodermal cell. Mesoglea (m, yellow dashed line) separating the two cell layers is shown for reference.* ***E)*** *SEM image of the aboral pole of a larva and its apical organ (ao, inside dashed ring). Note the different appearance of the ciliated ectodermal surface.*

These two examples demonstrate that there is high temporal variability and spatial patchiness within the ciliary response. Using recordings of other larvae not illustrated here, we generally observed that cilia at the oral pole were quickest to arrest after the light-off change, and that the beating stops gradually or in patches, propagating towards the aboral pole. Together with the flowfield measurements, we can be confident that a near-total ciliary arrest occurs quite consistently, and that this results in complete cessation in flow (larval swimming). The surface of the coral larva is completely covered in cilia, which protrude from many thousands of long, narrow (monociliated) ectodermal cells (Fig. 4D). There was often a small population of cilia at the very top of the aboral pole, perhaps associated with the apical organ (Fig. 4E) that never stopped beating. The cilia may, or may not recover their beating again within 100 s of the initial arrest when left in dim red light.

Body shape changes

Individual larvae of the same age, developmental stage and batch can vary considerably in overall size, shape and eccentricity. Generally by 5-6 dpf, the body has elongated to a bullet-shape, often with slightly wider profile at the aboral (anterior) pole.

All larvae (n=12) demonstrated dark-induced shape changes during the light-off experiment, by gradually contracting the longitudinal muscles and shortening their body length along the oral-aboral axis. This resulted in a reduction of length/width ratio. This shortening resulted in a rounder shape with some widening across the middle of the larvae with axis perpendicular to the oral-aboral axis. This significantly changed the eccentricity (width to length aspect ratio) of the larvae (Wilcoxon rank sum test, W=1059, p=0.001 for 2021, W=551, p<0.001 for 2022) (Fig. 5A) and also, to a lesser extent, the 2-dimensional area of the larval profiles (Wilcoxon rank sum test, W=1262, p=0.04 for 2021, W=716, p<0.001 for 2022) (Fig. 5B) (statistics in Table S3). Generally, the response showed good reproducibility and in most larvae, the change was striking (see example in Fig. 5C). However, one larva from 2021 spawning showed a very weak response to the first and third dark periods, suggesting that the response may not occur consistently. The two cohorts of larvae measured generally within the same size range, although larvae spawned in 2022 displayed greater changes than the previous year. The response can be watched in Video S2 and Video S6, where two larvae (one from each cohort) are exemplified.

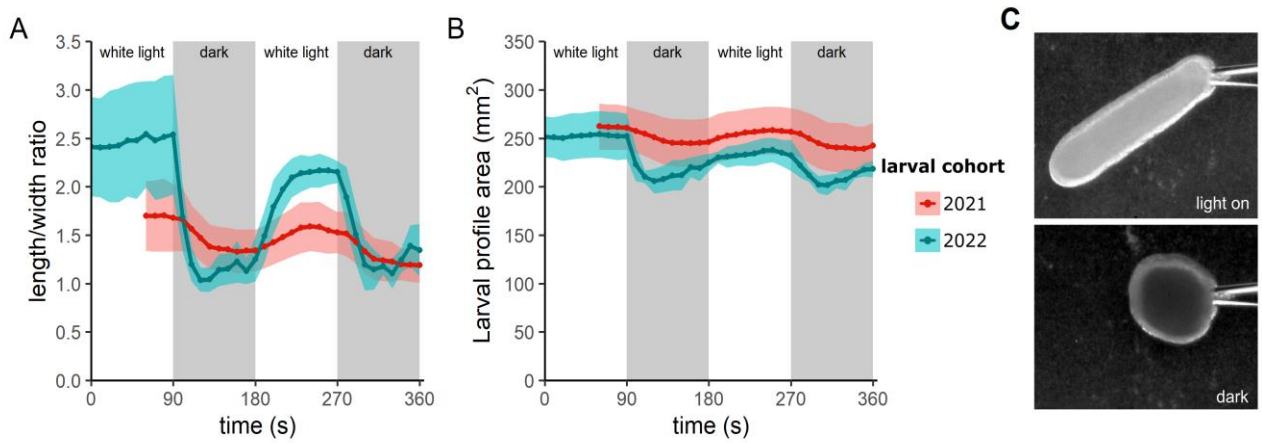

Figure 5. Larval body contractions and shape change in response to decrease in white light intensity. *Data are shown for individuals measured in 2021 (red) and 2022 (blue) as a mean of 6 individuals per cohort, with shading to indicate confidence intervals of the mean. 90 sec bright white light periods were alternated with 90 sec dark periods, which are indicated by grey background shading. Note, individuals from 2021 were not recorded for the first 60 s of the first light period.* ***A)*** *Eccentricity changes as a ratio of length (along oral-aboral axis) divided by width (perpendicular to the oral-aboral axis) are represented over time.* ***B)*** *The projected area of the larval profiles as they appear in the video.* ***C)*** *An example of a larva held on a suction micropipette near its oral opening, elongated during exposure to bright white light at the beginning of the experiment (top). The same larva is shown again after 60 seconds into a dark phase (bottom) and its body is contracted in length to form a spherical shape.*

Vertical positioning

To assess the natural buoyancy of larvae, we removed the cilia using a brief exposure to hyperosmotic seawater. This made them unable to swim and actively modulate their own position in the water column. After mixing to distribute the larvae inside a tall (44 mm) and narrow (10 x 10 mm) glass cuvette filled with artificial seawater, almost all larvae floated upwards within 50 s (trajectories shown in Fig. 6A, example in Video S7, panel A). This is demonstrated by the high proportion of larvae (3 batches, total n=100) moving in an upwards direction (Fig. 6B) in the seconds after mixing, in addition to a positive vertical displacement of 0.5 mm/s (Fig. 6C). This indicates that our *A. millepora* larvae were positively buoyant in seawater at this developmental stage of 4 dpf.

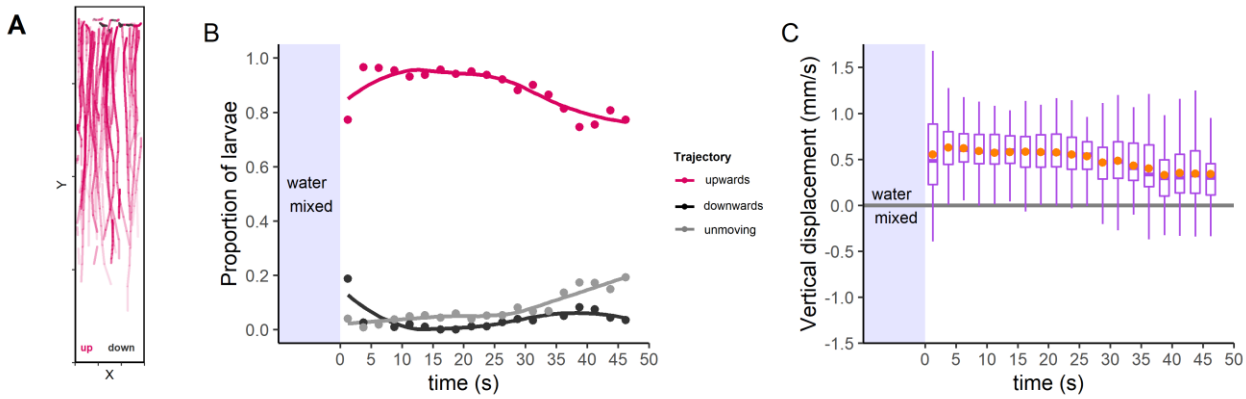

Figure 6. Vertical trajectories of larvae with swimming cilia removed. *Data are averaged from three batches containing a total of n=96 tracked larvae.* ***A)*** *Example batch showing trajectories of larvae over time. Red lines show movement upwards in the cuvette whereas black shows downwards movement, and increasing time is shown by increasing weight (alpha value) of that line.* ***B)*** *Mean proportion of larvae moving upwards (red), downwards (black) or neither (grey) after mixing.* ***C)*** *Vertical displacement as boxplots, with mean values overlaid (orange points). Positive values indicate net upward movement.*

To test the hypothesis that the ciliary arrest and body rounding response to darkness results in a similar upwards movement of the larvae, we subjected them to 90 s on/off periods of bright white light and tracked their vertical position in the same cuvette. Larval swimming speed showed similar trends to our horizontal cuvette assay, where speed significantly reduced during the dark periods (Wilcoxon rank sum test, W=52652241, $p<0.001$) (Supplementary Table S4, Fig. S4).

In the first light-on period, the proportion of larvae swimming up and down were relatively similar as they explored the cuvette (Fig. 7) and this period was therefore excluded from statistical testing. However, when the light stimulus was turned off, over half of the larvae showed net upward movement in darkness. In the following light phase, the proportion of larvae moving in a downward direction became dominant (>0.5), before a return to upward movement in the final dark phase. It should be noted that the mean distances travelled were small and vertical displacement shows only a weak, but significant trend of upward movement in the dark, and downwards movement in the second light phase (Wilcoxon rank sum test, W=87668661, $p<0.001$). Batch 1 was an exception to this trend and showed no difference between light and dark phase vertical displacement (See supplementary Table S5 and Figs. S5 & S7 for full results). Larvae closest to the bottom surface of the cuvette tended to exhibit a probing behaviour on the bottom in the light-on phase (Video S7, panel B). Then in the dark period, larvae in the bottom region became relatively still and floated very gradually upwards (Video S7, panel C). Larvae further up in the water column tended not to respond to the light dimming as often.

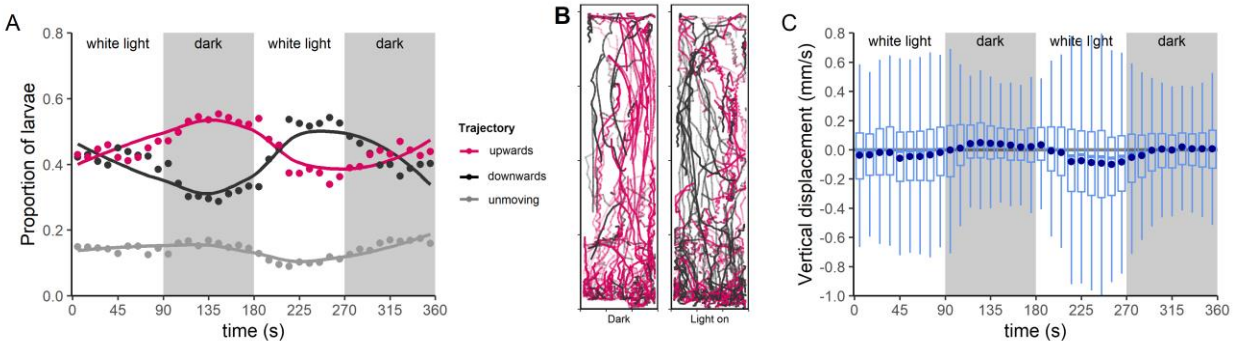

Figure 7. Vertical trajectories of larvae in the cuvette's water column during on/off periods of bright white light and darkness. *Data are averaged from six batches containing a total of n=361 tracked larvae. Grey shaded areas represent the two periods of darkness in time* ***A)*** *Mean proportion of larvae moving upwards (red), downwards (black) or neither (grey).* ***B)*** *Example batch showing trajectories of larvae over time in the first dark period (91-180 s) and following light period (181-270 s). Red lines show movement upwards in the cuvette whereas black shows downwards movement, and increasing time is shown by increasing weight (alpha value) of that line.* ***C)*** *Vertical displacement as boxplots, with mean values overlaid (dark blue points). Positive values indicate net upward movement, whereas negative values indicate downward net movement.*

Figure 7B shows an example batch (#2) with a proportionally greater number of smooth upward trajectories (red) indicating passive movement upwards, compared with the following dark phase. In the dark, active downward movement is dominant, shown by the increased amount of black helical tracks, concentrated at the bottom of the cuvette. Note, the large amount of variation in general swimming behaviour, likely due to a portion of larvae who did not respond to the light dimming, retaining relatively fast movement and adding considerable noise to the data. The light-off phases were characterised by very slow and likely passive movement, with smaller distances travelled. The vertical displacement (Fig. 7C) does not reach the large positive values of deciliated larvae (Fig. 6B, see Video S7) and there is not a net migration to the top of the cuvette in the dark periods. This suggests that the cilia are perhaps important for maintaining position in the water column during periods of dark-induced contraction.

Discussion

We show here that coral larvae of *A. millepora* exhibit a behavioural response to sudden light dimming by contracting the body and becoming rounded in shape (Video S2). They also reduce swimming speed, which is, at least in part, caused by an arrest of the swimming cilia. We found no evidence of phototaxis, but larvae may be capable of directional swimming up and down in the vertical plane, using gravitaxis [29,30]. We propose that these behaviours are important for maintaining position within the sunlit areas of a reef when exploring habitats for settlement, as we shall explain.

Our results for swimming speed reductions and lack of phototaxis behaviour were consistent with that for another acroporid coral larva, *A. tenuis* [27]. The mean free-

443 swimming speed (0.41 ±0.43 mm/s) under bright white light in our shallow cuvette was
444 lower than that reported for *A. tenuis* (1.96 ±0.8 mm/s [27]), but this is mostly likely due to
445 larger body size of *A. millepora* larvae, in addition to our use of a relatively smaller arena.
446 Larvae made more frequent contact with its edges, unable to reach the speeds that they
447 would otherwise achieve in larger water volumes. However, the maximum speed recorded
448 from a single larva in the first bright light phase was 2.0 mm/s, suggesting that this species
449 can swim at comparable speeds to *A. tenuis.*

450 The muscular and ciliary light-off responses are robust, however not always consistent.
451 There were occasionally individuals that did not respond every time, or at all, during tests.
452 Internal states (affecting "motivation") may explain this because larvae were disturbed and
453 handled via pipette tips prior to experiments, or directly tethered with a glass suction
454 pipette. This may have occasionally caused a stress or escape response to supersede the
455 light response. We also acknowledge the unnatural conditions of a small confined arena
456 containing a high density of larvae, which meant collisions could happen relatively
457 frequently, compared to the open ocean environment they are adapted to.

458 After the light is dimmed, a delay usually follows before there is a response in either the
459 muscular rounding or ciliary arrest responses. The larva may be sampling light over a
460 period of several seconds to integrate an average intensity signal and filter out rapid
461 changes. These include caustic flicker (dynamic patterns of light and shadow created by the
462 refraction and reflection of sunlight as it passes through a rippling water surface [31]) and
463 animals such as fish that cast a shadow below them. Or, the short (several second) dimming
464 periods resulting from swimming under a small object such as a coral branch.

465 In the *A. millepora* larva, there are two separate mechanisms that appear to occur together.
466 Ectodermal cilia form metachronal waves to spin and propel the coral larva through the
467 water [32]. In other ciliated marine invertebrate larvae such as the *Platynereis* worm,
468 ciliary closures are coordinated in the nervous system with distinct ciliomotor neuronal
469 circuitry [33,34]. Perhaps cnidarians lack such nervous system organisation for ciliary
470 arrest, and it is not known whether the muscles in the planula are controlled with separate
471 motor neurons or not. From our observations while imaging the cilia fields, ciliary closures
472 do not happen all over the body at once. Rather, they appeared to arrest first at the oral
473 pole, then patches of cilia gradually stopped, the stillness spreading aborally over the
474 subsequent few seconds, sometimes taking a minute. Those on the very end of the aboral
475 pole (perhaps apical organ cells' cilia, shown in Fig. 4E), seemed to continue beating in the
476 dimmed conditions, which may explain the phenomenon seen in our shallow cuvette assay
477 where free-swimming larvae gently spun on their own axis. The rate of ciliary arrest
478 propagation across the larval ectoderm that we observed from larva #2 was 23.3 μm/s
479 (from calculating the slope of the spread in distance/time). This relatively slow, patchy
480 spread of ciliary response we observed suggests a fairly crude, slow-acting nervous system
481 control, likely mediated with neuropeptide signalling [34,35].

482 Muscular involvement in swimming behaviour may have evolved later than ciliated
483 swimming in marine microswimmers [36]. The muscular contraction response is also slow
484 and patchy. We did not see a fast, simultaneous and smooth shortening across the body,
485 rather groups of muscles contract in events at different times (see video S6). This suggests

that a slow-spreading signalling mechanism such as a diffusing neuropeptide may be involved in this process too [35].

Expression patterns of opsins reveal that the planulae of coral and other anthozoans have photoreceptors speckled across the ectoderm or endoderm [22,37], rather than tightly clustered into eye-like spots. Therefore, there is no viable system for spatial vision or even detecting the direction of oncoming light [38]. Thus, the coral larva is unable to "see" where it is going when exploring the reef and cannot predict the light environment they are swimming toward.

The coral reef is a complex, layered and highly structured environment where adult colonies of numerous coral species grow in various directions to capture available down-welling light [39]. Among the dead and living coral structures, crevices and overhangs are interspersed, creating dark spaces within the reef, which would be unsuitable for survival of new coral recruits. Abundance and spectral quality of light is one of the factors effecting distinct depth zonation in coral species communities [10,40,41], which is mediated by both larval choice [9,12–16] and subsequent growth and survival of the adult [41–43]. To locate an optimal settlement site in this habitat, larvae must use a variety of sensory cues, including light availability. Too shallow, and the colony would be exposed to harmful ultraviolet radiation and wave action [44], and too deep or shaded would limit zooxanthellate symbiont recruitment and photosynthetic output. Thus, the coral larva must navigate a habitat with a depth-light gradient and smaller-scale structures creating more extreme light gradients via shading. The sudden light-off conditions we used in our experiments may simulate an individual's travel from bright sunlit surface into a dark crevice or overhang (Fig. 8). Based on a swimming speed of 1.0 mm/s and a light-off response delay of 15 s, without ambient water flow the larva would travel just 15 mm before stopping its trajectory any further into the dark environment. The rounded shape and tendency for the larva to spin gently on its axis may serve as a useful method to change direction, quite randomly of course, as they are unable to sense light direction (Fig. 8, top right panel). Random orientation changes are common navigation strategies among some motile unicellular organisms, such as bacteria and some protists that perform random-walk chemotaxis [45]. In the eyeless coral larva, we propose that their simple scotophobic response system allows some control on positioning with respect to light environment. Trial and error would lead them eventually to a suitable settlement site. Like *A. tenuis* [27], during prolonged periods of darkness (2-3 minutes), the larvae of *A. millepora* do eventually elongate and resume exploratory swimming. Therefore, they may eventually be able to find their way out of a dark area again.

In the vertical cuvettes (refer to Video S7), larvae that stayed in close proximity to the base of the chamber were presumably probing the surface in search of cues for a settlement site. In the following dark period, it was these individuals that responded most consistently to the light dimming by stopping their active swimming and floating almost motionless (we can assume that they rounded in shape too). However, larvae higher in the column often continued to swim actively and did not show the light-off response consistently. This suggests that the light-off response we describe is perhaps only activated when the larva is in association with a surface, when it would be searching for a suitable settlement site.

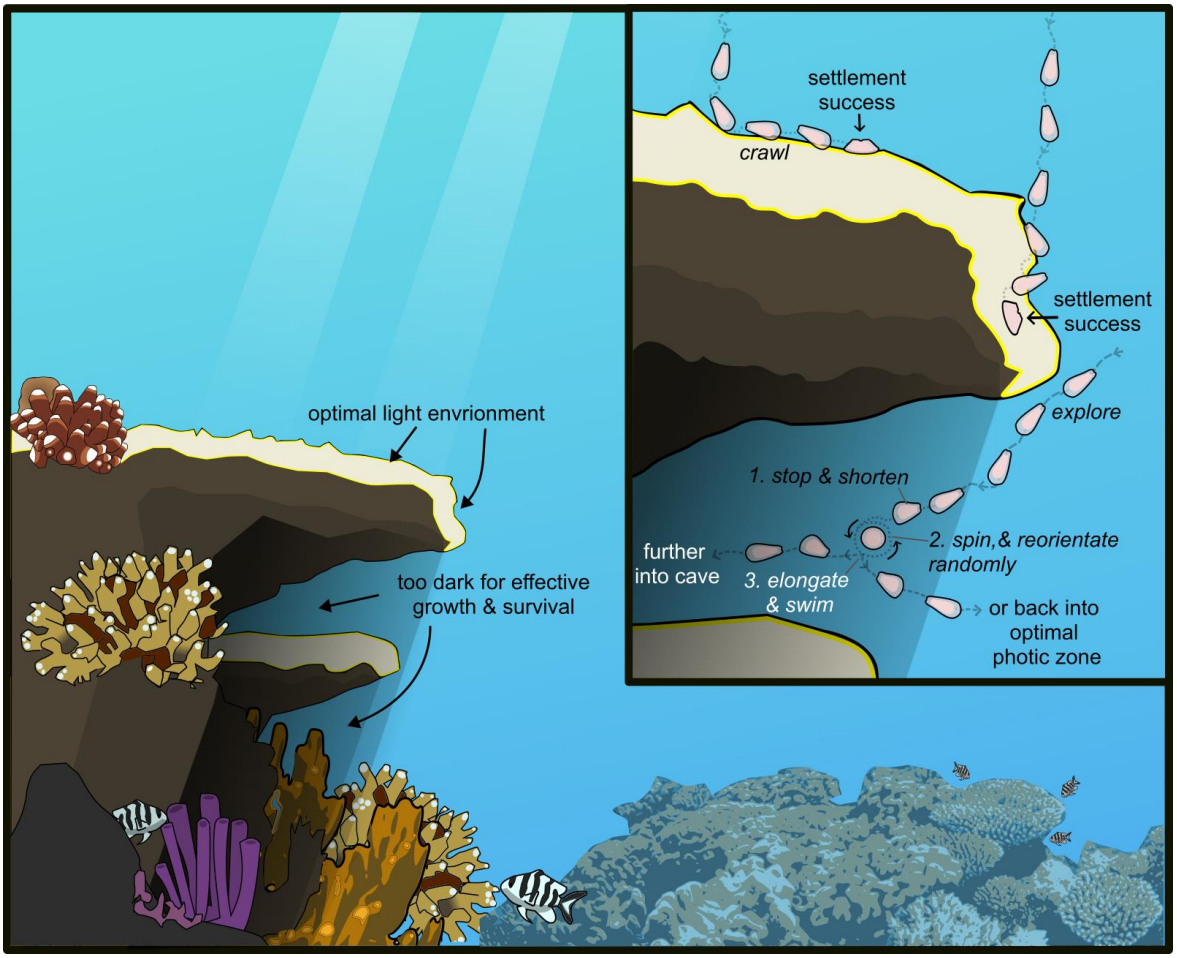

Figure 8. Schematic of Acropora larva movement in situ on a highly structured coral reef. *The larvae are likely to explore lit and shaded areas in search of a settlement site. Their scotophobic behvioural response to sudden perceived light dimming may allow them to maintain position in the lit areas without directional light sensing or vision.*

To our knowledge, this is the first report of a body-rounding behavioural response to light dimming in coral larvae. This study leaves us with many more questions and avenues for further study. For example, we would be interested to know how very gradual light dimming encountered with swimming downwards along a depth-light gradient might affect the larva's swimming behaviour once it reached an intensity threshold. The neural mechanisms of the light-off response and the biophysical mechanism of coupling between muscles and cilia also remain unclear.

Acknowledgements

This work was funded by the Human Frontiers Science Program (HFSP) grant No. RGP0033/2020. This project has also received funding from the European Research Council (ERC) under the European Union's Horizon 2020 research and innovation programme (Grant Agreement No. 101020792 to GJ and No. 853560 to KYW).

We would like to thank Dr. Jamie Craggs and colleagues at the Horniman Museum and Gardens aquarium facility and the Coral Spawning Lab for providing us with live coral larvae. Thank you also to Prof. Nick Roberts from the Ecology of Vision Lab, Bristol for lending us a spectrometer.

References

1. Sorokin YI. 1973 Trophical role of bacteria in the ecosystem of the coral reef. *Nature* **242**, 415–417. (doi:10.1038/242415a0)

2. Hejnol A *et al.* 2009 Assessing the root of bilaterian animals with scalable phylogenomic methods. *Proceedings of the Royal Society B: Biological Sciences* **276**, 4261–4270. (doi:10.1098/rspb.2009.0896)

3. Genikhovich G, Technau U. 2017 On the evolution of bilaterality. *Development* **144**, 3392–3404. (doi:10.1242/dev.141507)

4. Satterlie R. 2019 Cnidarian neurobiology. pp. 184–218. Oxford University Press. (doi:10.1093/oxfordhb/9780190456757.013.7)

5. Maida M, Coll JC, Sammarco PW. 1994 Shedding new light on scleractinian coral recruitment. *Journal of Experimental Marine Biology and Ecology* **180**, 189–202. (doi:10.1016/0022-0981(94)90066-3)

6. Harrington L, Fabricius K, De'ath G, Negri A. 2004 Recognition and selection of settlement substrata determine post-settlement survival in corals. *Ecology* **85**, 3428–3437. (doi:10.1890/04-0298)

7. Ricardo GF, Jones RJ, Nordborg M, Negri AP. 2017 Settlement patterns of the coral *Acropora millepora* on sediment-laden surfaces. *Science of the Total Environment* **609**, 277–288. (doi:10.1016/j.scitotenv.2017.07.153)

8. Pysanczyn JW, Williams EA, Brodrick E, Robert D, Craggs J, Marhaver KL, Simpson SD. 2023 The role of acoustics within the sensory landscape of coral larval settlement. *Frontiers in Marine Science* **10**. (doi:10.3389/fmars.2023.1111599)

9. Mundy CN, Babcock RC. 1998 Role of light intensity and spectral quality in coral settlement: Implications for depth-dependent settlement? *Journal of Experimental Marine Biology and Ecology* **223**, 235–255. (doi:10.1016/S0022-0981(97)00167-6)

10. Roberts TE, Bridge TCL, Caley MJ, Madin JS, Baird AH. 2019 Resolving the depth zonation paradox in reef-building corals. *Ecology* **100**, e02761. (doi:10.1002/ecy.2761)

11. Quigley KM, Strader ME, Matz MV. 2018 Relationship between *Acropora millepora* juvenile fluorescence and composition of newly established symbiodinium assemblage. *PeerJ* **6**, e5022. (doi:10.7717/peerj.5022)

12. Gleason DF, Edmunds PJ, Gates RD. 2006 Ultraviolet radiation effects on the behavior and recruitment of larvae from the reef coral *Porites astreoides*. *Marine Biology* **148**, 503–512. (doi:10.1007/S00227-005-0098-Y)

13. Mason B, Beard M, Miller MW. 2011 Coral larvae settle at a higher frequency on red surfaces. *Coral Reefs* **30**, 667–676. (doi:10.1007/s00338-011-0739-1)

14. Strader ME, Davies SW, Matz MV. 2015 Differential responses of coral larvae to the colour of ambient light guide them to suitable settlement microhabitat. *Royal Society Open Science* **2**. (doi:10.1098/RSOS.150358)

15. Foster T, Gilmour JP. 2016 Seeing red: Coral larvae are attracted to healthy-looking reefs. *Marine Ecology Progress Series* **559**, 65–71. (doi:10.3354/MEPS11902)

16. Ricardo GF, Harper CE, Negri AP, Luter HM, Abdul Wahab MA, Jones RJ. 2021 Impacts of water quality on *Acropora* coral settlement: The relative importance of substrate quality and light. *Science of The Total Environment* **777**, 146079. (doi:10.1016/J.SCITOTENV.2021.146079)

17. Levy O, Appelbaum L, Leggat W, Gothlif Y, Hayward DC, Miller DJ, Hoegh-Guldberg O. 2007 Light-responsive cryptochromes from a simple multicellular animal, the coral *Acropora millepora*. *Science* **318**, 467–470. (doi:10.1126/science.1145432)

18. Gorbunov MY, Falkowski PG. 2002 Photoreceptors in the cnidarian hosts allow symbiotic corals to sense blue moonlight. *Limnology and Oceanography* **47**, 309–315. (doi:10.4319/lo.2002.47.1.0309)

19. Vize PD. 2009 Transcriptome analysis of the circadian regulatory network in the coral *Acropora millepora*. *Biological Bulletin* **216**, 131–137. (doi:10.2307/25470735)

20. Gornik SG, Bergheim BG, Morel B, Stamatakis A, Foulkes NS, Guse A. 2021 Photoreceptor diversification accompanies the evolution of Anthozoa. *Molecular biology and evolution* **38**, 1744–1760.

21. Boch CA, Ananthasubramaniam B, Sweeney AM, Doyle FJ, Morse DE. 2011 Effects of light dynamics on coral spawning synchrony. *The Biological Bulletin* **220**, 161–173. (doi:10.1086/BBLv220n3p161)

22. Mason B, Schmale M, Gibbs P, Miller MW, Wang Q, Levay K, Shestopalov V, Slepak VZ. 2012 Evidence for multiple phototransduction pathways in a reef-building coral. *PLOS ONE* **7**, e50371. (doi:10.1371/JOURNAL.PONE.0050371)

23. Mason BM, Koyanagi M, Sugihara T, Iwasaki M, Slepak V, Miller DJ, Sakai Y, Terakita A. 2023 Multiple opsins in a reef-building coral, *Acropora millepora*. *Scientific Reports* **13**, 1628. (doi:10.1038/s41598-023-28476-5)

24. Mulla AJ, Lin C-H, Takahashi S, Nozawa Y. 2021 Photo-movement of coral larvae influences vertical positioning in the ocean. *Coral Reefs 2021 40:4* **40**, 1297–1306. (doi:10.1007/S00338-021-02141-7)

25. Kawaguti S. 1941 On the physiology of reef corals V. Tropisms of coral planulae, considered as a factor of distribution of the reefs. *Palao Tropical Biological Station Studies* **2**, 319–328.

26. Lewis JB. 1974 The settlement behaviour of planulae larvae of the hermatypic coral *Favia fragum* (Esper). *Journal of Experimental Marine Biology and Ecology* **15**, 165–172. (doi:10.1016/0022-0981(74)90042-2)

27. Sakai Y *et al.* 2020 A step-down photophobic response in coral larvae: implications for the light-dependent distribution of the common reef coral, *Acropora tenuis*. *Scientific Reports* **10**. (doi:10.1038/s41598-020-74649-x)

28. R Core Team. 2021 *R: A language and environment for statistical computing*. Vienna, Austria: R Foundation for Statistical Computing. See https://www.R-project.org/.

29. Takeda-Sakazume A, Honjo J, Sasano S, Matsushima K, Baba SA, Mogami Y, Hatta M. 2022 Gravitactic swimming of the planula larva of the coral *Acropora*: Characterization of straightforward vertical swimming. *Zoological Science* **40**, 44–52. (doi:10.2108/zs220043)

30. Arai I, Kato M, Heyward A, Ikeda Y, Iizuka T, Maruyama T. 1993 Lipid composition of positively buoyant eggs of reef building corals. *Coral Reefs 1993 12:2* **12**, 71–75. (doi:10.1007/BF00302104)

31. McFarland WN, Loew ER. 1983 Wave produced changes in underwater light and their relations to vision. *Environmental Biology of Fishes* **8**, 173–184. (doi:10.1007/BF00001083)

32. Poon RN, Westwood TA, Laeverenz-Schlogelhofer H, Brodrick E, Craggs J, Keaveny EE, Jékely G, Wan KY. 2023 Ciliary propulsion and metachronal coordination in reef coral larvae. *Physical Review Research* **5**, L042037. (doi:10.1103/PhysRevResearch.5.L042037)

33. Verasztó C, Ueda N, Bezares-Calderón LA, Panzera A, Williams EA, Shahidi R, Jékely G. 2017 Ciliomotor circuitry underlying whole-body coordination of ciliary activity in the *Platynereis* larva. *eLife* **6**, e26000. (doi:10.7554/eLife.26000)

34. Marinković M, Berger J, Jékely G. 2020 Neuronal coordination of motile cilia in locomotion and feeding. *Philosophical Transactions of the Royal Society B: Biological Sciences* **375**, 20190165. (doi:10.1098/rstb.2019.0165)

35. Jékely G, Yuste R. 2024 Nonsynaptic encoding of behavior by neuropeptides. *Current Opinion in Behavioral Sciences* **60**, 101456. (doi:10.1016/j.cobeha.2024.101456)

36. Jékely G. 2011 Origin and early evolution of neural circuits for the control of ciliary locomotion. *Proceedings of the Royal Society B: Biological Sciences* **278**, 914–922. (doi:10.1098/rspb.2010.2027)

37. McCulloch KJ, Babonis LS, Liu A, Daly CM, Martindale MQ, Koenig KM. 2023 *Nematostella vecten*sis exemplifies the exceptional expansion and diversity of opsins in the eyeless Hexacorallia. *EvoDevo* **14**, 14. (doi:10.1186/s13227-023-00218-8)

38. Brodrick E, Jékely G. 2023 Photobehaviours guided by simple photoreceptor systems. *Animal Cognition* **26**, 1817–1835. (doi:10.1007/s10071-023-01818-6)

39. Guendulain-García SD, Lopez-Beltran A, Banaszak AT, Álvarez-Filip L, Ramírez-Chávez E, García-Medrano D, Sellares-Blasco R, López-Pérez A. 2023 Photogrammetry for coral structural complexity: What is beyond sight? *Coral Reefs* **42**, 635–644. (doi:10.1007/s00338-023-02368-6)

40. Lesser MP, Slattery M, Leichter JJ. 2009 Ecology of mesophotic coral reefs. *Journal of Experimental Marine Biology and Ecology* **375**, 1–8. (doi:10.1016/j.jembe.2009.05.009)

41. Tamir R, Eyal G, Kramer N, Laverick JH, Loya Y. 2019 Light environment drives the shallow-to-mesophotic coral community transition. *Ecosphere* **10**, e02839. (doi:10.1002/ecs2.2839)

42. Vermeij M, Bak R. 2002 How are coral populations structured by light? Marine light regimes and the distribution of Madracis. *Marine Ecology Progress Series* **233**, 105–116. (doi:10.3354/meps233105)

43. Hennige SJ, Smith DJ, Walsh S-J, McGinley MP, Warner ME, Suggett DJ. 2010 Acclimation and adaptation of scleractinian coral communities along environmental gradients within an Indonesian reef system. *Journal of Experimental Marine Biology and Ecology* **391**, 143–152. (doi:10.1016/j.jembe.2010.06.019)

44. Lesser MP. 1997 Oxidative stress causes coral bleaching during exposure to elevated temperatures. *Coral Reefs* **16**, 187–192. (doi:10.1007/S003380050073)

45. Wan KY, Jékely G. 2021 Origins of eukaryotic excitability. *Philosophical Transactions of the Royal Society B: Biological Sciences* **376**, 20190758. (doi:10.1098/rstb.2019.0758)